Article:

Garcia-Taengua, E, Martí-Vargas, JR and Serna, P (2014) Splitting of concrete cover in steel fiber reinforced concrete: Semi-empirical modeling and minimum confinement requirements. Construction and Building Materials, 66. pp. 743-751. ISSN 0950-0618

https://doi.org/10.1016/j.conbuildmat.2014.06.020

Splitting of Concrete Cover in Steel Fiber Reinforced Concrete: Semi-Empirical Modelling and Minimum Confinement Requirements.

E. García-Taengua[1]*, J.R. Martí-Vargas[2], P. Serna[3]

[1] School of Planning, Architecture and Civil Engineering, Queen's University, Belfast, Northern Ireland, United Kingdom.

[2-3] ICITECH-Institute of Concrete Science and Technology, Universitat Politècnica de València, Valencia, Spain

e-mail addresses: e.garcia-taengua@qub.ac.uk, jrmarti@cst.upv.es, pserna@cst.upv.es

***Corresponding author:** e.garcia-taengua@qub.ac.uk

ABSTRACT

The use of steel fiber reinforced concrete (SFRC) is becoming more and more common. Concerning bond of rebars to concrete, fibers provide passive confinement and not only improve bond performance but also affect the mode of bond failure. To analyze these aspects, a series of prismatic specimens have been subjected to the Pull Out Test, and an accurate model for predicting the mode of bond failure has been developed. The following factors have been considered: concrete compressive strength (30-50 MPa), rebar diameter (8-20 mm), concrete cover (between 30 mm and 5 times rebar diameter), fiber content (up to 70 kg/m^3), and fiber slenderness and length. This model relates splitting probability to the factors considered. It has been proved that increasing fiber content restrains the risk of splitting failure. The favorable effect of fibers when preventing splitting failures has been revealed to be more important for higher concrete compressive strength values, which require higher concrete cover/diameter ratios for splitting failure to be prevented. Fiber slenderness and fiber length modify the effect of fiber content on splitting probability and therefore on minimum cover/diameter ratios required to prevent splitting failures.

KEYWORDS:

concrete, fiber, confinement, splitting, bond, model, failure

1. INTRODUCTION

This section describes the phenomena involved in bond of rebars to concrete and reviews previous literature concerned with the role of fibers. For a better understanding, this information is organised in three different subsections. The first one presents an overview of the mechanisms controlling bond of rebars to concrete. Then, the second subsection deals with the different modes of bond failure and puts splitting failures in context, paying special attention to the role of passive confinement. Finally, the role of fibers in relation to bond and specially splitting failures is exposed. All this information contextualizes the topic under study and justifies the objectives of this study, which are detailed right after that.

1.1 Bond of Reinforcing Bars to Concrete

Bond between reinforcement and concrete is commonly conceptualized as a shear stress, or bond stress, distributed over the surface of the rebar along the embedded length. Bond stress can be defined as the ratio between the rate of change in axial force along the rebar and the area of rebar surface over which this change takes place [1]. However, there are other aspects besides bond stress to be considered, especially in the case of deformed, ribbed rebars [1–3], mainly related to radial stresses.

As Figure 1 shows, the tensile load pulling the rebar out of concrete produces reaction forces which are exerted on the sorrounding concrete by ribs. These reactions can be decomposed in two components and therefore, the bond phenomenon involves: a) a shear component, parallel to the rebar axis, so that there are triaxially compressed concrete regions in front of each rib, and b) a radial component, orthogonal to the shear component, which extends bond mechanisms to the surrounding concrete.

As the axial load on the rebar increases, the wedging action by rebar ribs increases and concrete between ribs is crushed. At the same time, the derived radial stresses are also increased and concrete tensile strength is reached in the surrounding concrete. This leads to the phenomenon of transverse microcracking which is at the very basis of the loss of strain compatibility between rebar and concrete: relative displacement of the rebar with respect to concrete (slip) increases as a result of the widening of these microcracks.

Progress of the rebar slip implies activation of bond and progressive increase of bond stresses until the bond strength is reached. Bond stress–slip curves are characterized by postpeak softening behavior: bond stress remains remarkable even at very large slips in the postpeak region [4], and slippage represents shear fracture [5].

Consequently, because of both shear and radial components, and based on confinement conditions, bond failure can occur in two different major modes. One mode consists in splitting of concrete surrounding the rebar (splitting failure), and the other mode consists in having the rebar pulled out after the shear failure of the steel-concrete interface (pullout failure).

1.2 Modes of Bond Failure and Passive Confinement

Confinement plays a major role as a parameter affecting bond. A distinction is made between active and passive confinement. Active confinement is the consequence of concrete being compressed by external forces, for instance reactions in supports or beam-column joints. Passive confinement is the constraining effect that results from concrete cover and transverse reinforcement. This constraining effect is progressively activated with the onset of bond stresses.

Splitting failures occur when concrete is not well confined. Transverse cracks originated at the rebar-concrete interface may eventually reach concrete surface, and if there is no transverse reinforcement capable of bearing the derived tensile stresses, bond capacity is totally lost in a brittle failure followed by a considerable slippage.

Pullout failures, on the other hand, occur when confinement prevents these cracks from reaching concrete surface. The concrete crushed between ribs, which defines a cylindrical frictional surface around the rebar [6], is extracted with the rebar. After the shearing has progressed over the entire length of embedment of the rebar, the force drops and then the remaining pullout is resisted only by friction.

Passive confinement includes not only the effect of concrete cover but also that of transverse reinforcement, and is treated in similar ways by different codes. The major concern regarding passive confinement is connected to the minimum values of transverse reinforcement or concrete cover in order to prevent concrete splitting [7]. According to the Model Code [8], concrete is considered well confined when concrete cover is not less than five times the rebar diameter. The minimum concrete cover value to avoid splitting failures is approximately between 2.5 and 3.0 times rebar diameter [9, 10].

The confining effect of concrete cover is most usually typified by rebar diameter: concrete cover/diameter ratio is the reference parameter, because the effect of concrete cover is inversely related to rebar diameter. Passive confinement affects bond performance in terms of bond strength and bond failure ductility as well [7], not only in relation to the mode of bond failure [11, 12]. Furthermore, bond stress–slip curves become steeper as concrete cover increases (FIB 2000): concrete confinement in the splice/development region improves the ductility of bond failure as well [13].

1.3 Bond of Reinforcing Bars to Steel Fiber Reinforced Concrete (SFRC)

Fibers have a positive effect on bond of reinforcement to concrete, even when low fiber contents are considered [14]. Fibers improve bond performance because they confine reinforcement (playing a similar role to that of the transverse reinforcement) and because they broaden the range of crack width values within which passive confinement remains active [14–16]. Improvements in bond performance of concrete are really important in terms of toughness and ductility of the material [13, 17].

In particular, the Spanish code for structural concrete [18] explicitly states that fibers improve bond capacity of concrete and that this can be taken into account when designing anchors and splices. Similar statements are found in the recommendations by other organisms [10, 19].

However, the positive effect of fibers is acknowledged but is not always explicitly introduced in formulations for anchorage/splice lengths. Considering that the use of non-conventional concretes, including steel fiber reinforced concrete (SFRC hereafter), is becoming more and more common [20–22], it is likely that anchorage lengths are higher than necessary in most of the cases. How to take advantage of the higher ductility and energy absorption capacity of SFRC to reduce anchorage lengths when using fibers is not a straightforward issue. In this sense, several studies have been performed attempting to model the bond phenomenon and anchorage behavior in general [23–30].

A central issue is whether the effect of fibers on bond is modified by concrete compressive strength and rebar diameter. Since large diameters increase the tendency to concrete cover splitting, an important issue is the study of the relationship between the presence of fibers and the concrete cover needed to prevent splitting failures. In fact, the effect of fibers on bond when there is splitting of the concrete cover proves to be very important [25, 31]. On the contrary, it is not so clearly significant when splitting does not occur: under such circumstances fibers have been reported to affect bond failure ductility but not bond strength.

The study how fibers determine mode of bond failure, and how they are related to concrete compressive strength and rebar diameter in terms of probability that no cover splitting occurs are issues that have not been addressed in scientific literature yet.

2. OBJECTIVES

The main objectives of this research have been:

- Deepening the knowledge of the phenomena involved in bond of reinforcement to Steel Fiber Reinforced Concrete (SFRC), especially regarding the role of fibers in relation to cover splitting and its prevention.
- Studying the effect of fiber geometry, fiber content, concrete compressive strength, and rebar diameter on minimum concrete cover values needed to prevent splitting failures.
- Obtaining analytical expressions which prove useful to estimate the risk or probability of splitting of the concrete cover in terms of the factors considered.
- Using the aforementioned analytical expressions to predict minimum confinement requirements that have to be met to avoid cover splitting on bond failure.

3. EXPERIMENTAL PROGRAMME

3.1 Factors and Levels Considered

The factors considered have been: concrete compressive strength (f_c), rebar diameter (D), concrete cover (C), steel fiber content (C_f), and fiber geometry (slenderness (λ_f) and length (l_f)).

The values or levels considered for each one of these factors are summarized in Table 1. To consider concrete compressive strength, three different reference mixes with compressive strength values between 30MPa and 50 MPa have been included. Each one of them has led to a group of different mixes as a result of adding fibers. Since they have been produced and tested sequentially, they have been numbered accordingly: all type I mixes were produced and tested in a first stage, then all type II mixes, and finally all type III mixes. They differ in terms of water/cement ratio, maximum aggregate size, and cement content, since this research is focused on normal strength concrete. The three reference mix designs considered in this research are summarized in Table 2.

Four different rebar diameters have been considered. 8mm rebars have been considered as representative of small rebars used in real applications (6mm and 8mm for building, 8mm and 10mm for civil engineering works). 16mm rebars have been selected because they are a commonplace in bond literature. At first (series with type I mixes) 20mm rebars were tested in addition to 8mm and 16mm diameters. However, after this first series, considering 8-12-16 mm diameters seemed more convenient than 8-16-20 mm. That is the reason why the values considered for rebar diameters are the same for type II and type III series but they differ from those for type I series (Table 3).

Concrete cover values have been defined as a function of rebar diameter. C1 is the smallest concrete cover value: in the first stage (type I series) it was 30 mmn, which is the minimum acceptable according to the Spanish code [18]. However, it was reset to 2.5 times the rebar diameter for type II and type III series, because this is usually assumed as the boundary distinguishing splitting failures and pullout failures. C3 is 5 times the rebar diameter in all cases, because this is the situation that the Model Code [8] defines as 'good confinement'. C2 was an intermediate value, $C1 < C2 < C3$: for type I series it was the average of C1 and C3, but for type II and type III series it was redefined as 3.5 times the rebar diameter.

Four types of hooked-end steel fibers have been considered which are different in terms of slenderness and length only: 45/50, 65/60, 80/35, and 80/50. They all are within the so-called macro-fibers and among the ones which are most widely used in precast industry.

Fiber contents considered have been decided below 1% in volume fraction (V_f) in addition to unreinforced concrete (0 kg/m^3), fiber contents from 40 kg/m^3 (V_f = 0.51%) to 60-70 kg/m^3 (V_f = 0.76-0.89%) constitute the referential frame for most usual SFRC applications.

3.2 Materials

Cement type CEM II/B-M 42.5 R was used in all cases. The aggregates used have been river sand, crushed limestone coarse aggregate, and limestone filler. The superplasticizer used has been a polycarboxylate ether. The reinforcing bars were type B 500 S. With respect to the steel fibers used, all of them are cold-drawn, hooked-end fibers made with low carbon steel (yield strength 1100 MPa minimum) and without any coating.

Each one of these reference mix designs was initially tested and adjusted to admit a volume fraction of 0.5% of 65/60 fibers with slump values between 10 cm and 15 cm. However, each one of these reference mix designs would be different in each particular case since fiber type and fiber content would differ according to their having been defined as factors. Consequently, filler and admixture amounts were adjusted in each case to keep slump values between 10 cm and 15 cm at the same time segregation was prevented.

3.3 Pull Out Test

A modified version of the Pull Out Test (POT) has been selected as the most appropriate test for the purposes of this research. Specimens for the POT have been designed based on the RILEM recommendations [32–34] which prescribes the following requirements: a) total length of the specimen (L) is to be 10 times the rebar diameter, though never less than 200 mm; and b) embedded length (L') is to be 5 times the rebar diameter, where the absence of sleeve protection allows the generation of bond stresses between rebar and concrete.

These conditions have been observed in all POT specimens produced and tested.

Preliminary calculations following Eurocode 2 (art. 8.4.2) [35] were made in order to avoid rebar yielding so that specimens failure could be related only to bond failure in all cases.

Specimens cross-section was defined as a function of rebar diameter and therefore varies depending on that parameter and on the concrete cover value considered in each particular case. Cross-section of POT specimens is sketched in Figure 3 in terms of the diameter of the rebar (D), the side (S), and the factor 'concrete cover', variable (C). As shown in Figure 3, rebar is positioned excentrically so that the factor 'concrete cover' is restricted to two out of four semi-axes in the cross-section. With respect to the other two semi-axes, concrete cover had to be greater in order to have a good confinement. According to the Model Code [8], it has a good confinement with concrete cover values bigger than 5 times the rebar diameter. It has been taken as reference a rebar diameter of 25 mm so that further research with bigger rebar diameters is compatible with all data obtained and reported herein. Accordingly, for the two semi-axes not considered as variable within the cross-section, a minimum dimension of $5 \cdot 25 = 125$ mm was established.

3.4 Design of the Experiment

In this case, a total of 5 factors (f_c, D, C, C_f, λ_f-l_f)) is under consideration, each one of them at 3 different values.

The selection of specimens to be produced and tested has followed a highly fractioned factorial plan [36] so that reliable, statistically sound conclusions can be obtained from experimental results after a reasonable number of tests.

The consideration given to concrete compressive strength as a factor is somewhat different with respect to how other factors have been handled when planning the experiment. It was more convenient to organize the highly fractioned factorial plan independently of concrete compressive strength, and then producing and testing all these combinations for type I series first, then for type II series, and then for type III series. The result is a fractional factorial design organized in blocks.

The combinations tested for each series resulting from the reference mixes are shown in Table 3. Each one of these combinations consisted of 3 POT specimens and 2 cylindrical specimens produced with concrete from the same batch. The number of POT specimens produced and tested is 9 x 3 = 27 for each series, and since there are 3 series, the total number of POT specimens in this research has been 27 x 3 = 81, far less than the 729 specimens that a complete experiment would have required.

3.5 Experimental methods

All concrete mixes in this research have been produced by following the same process and sequence in all cases.

Right after mixing, concrete slump was measured according to the standard EN 12350-2:2006. The criterion established for fresh mixes was that slump values ranged between 10 cm and 15 cm. Then, the concrete used was poured back to the mixer, and after 1 more minute mixing, POT specimens and cylindrical specimens were cast.

Each one of the batches of concrete produced was characterized by tesing under compression the two cylindrical specimens produced simultaneously with POT specimens. All cylindrical specimens were tested at the same age POT specimens were tested, i.e. 28 days. Test method to determine compressive strength was carried out according to EN 12390-2:2009.

Pull out tests were carried out as shown in Figure 4. The specimen to be tested was supported by a rigid steel plate with a hole in its center to allow the rebar passing through. The lower end of the rebar was anchored by clamps. By operating a hydraulic system the supporting plate was pulled up and, as a result, the rebar was pulled out of the specimen.

The slip of the rebar was monitored on the surface opposite to that from which the rebar was being pulled out by means of a LVDT sensor. It was located on this surface in order to detect the load corresponding to the onset of bond stress along the entire embedded length.

4. RESULTS

4.1 Concrete compressive strength

Concrete compressive strength average values obtained for type I, type II, and type III mixes were 32 MPa, 48 MPa, and 44 MPa respectively, obtained from cylindrical specimens tested at the age of 28 days. These average values have been used for the analysis of the results presented in following sections. The coefficient of variation has been 8.5%, 11% and 10.8%, respectively.

4.2 Mode of failure and bond strength

Table 3 shows the experimental results obtained, namely: the number of specimens out of each set of three that experienced cover splitting, and average bond strength values, calculated considering only those specimens that failed following a pullout mode. Bond strength values are shown for reference only. The variable subjected to analysis in the following sections is the count of splitting cases, because this paper focuses on the identification of variables that determine the mode of bond failure and the quantification of their effect on splitting risk.

5. ANALYSIS AND DISCUSSION

5.1 Development of a semi-empirical model to predict splitting risk

Logistic binary regression [37] has been used to relate the probability (p) of cover splitting in a POT specimen to the variables considered in this research (f_c, D, C, C_f, λ_f-l_f), This has been achieved by fitting a logistic equation to the experimental values obtained for p, which can be 0/3, 1/3, 2/3, or 3/3, shown in Table 3.

In this case, a semi-empirical logistic model has been obtained, so that it takes into account not only the experimental data obtained but also previous knowledge of bond phenomena. This helps interpreting the implications of the relations modelled and therefore adds value to the predictive tool.

This has been achieved by carefully pondering which interactions among the factors considered are likely to be at operation in relation to bond failure. Before fitting a logistic equation to the experimental data, the structure of this logistic equation has been tailored so that it better represents bond phenomena. As explained in the introduction, passive confinement plays a capital role on bond failure modes. If transverse reinforcement is not considered (as it is the case in this research), concrete cover/diameter ratio (C/D) is the main source of passive confinement. Therefore, it is reasonable to think that C/D is the only factor having a standalone effect on the risk of splitting, while its effect is modified by concrete properties. This implies the assumption that all other factors (compressive strength, fibers content and geometry) interact with, and therefore modify the effect of C/D ratio. This model is formulated by equation (1):

$$ln\left(\frac{p}{1-p}\right) = \nabla_0 + \left(\nabla_{cd} + \nabla_c f_c + \nabla_{\mathcal{F}} C_f\right)\frac{C}{D} \tag{1}$$

where ∇_0, ∇_{cd}, and ∇_c are coefficients to be estimated, and $\nabla_{\mathcal{F}}$ is a function of the geometry of fibers defined as follows:

$$\nabla_{\mathcal{F}} = \nabla_f + \nabla_{\lambda f}\lambda_f + \nabla_{\ell f}\ell_f \tag{2}$$

where ∇_f, $\nabla_{\lambda f}$, and $\nabla_{\ell f}$ are coefficients to be estimated.

The model thus formulated takes into account the nature of the phenomenon under study, and two aspects are particularly remarkable:

- The odds-ratio and therefore splitting probability are assumed to be mainly determined by C/D ratio, and the effect of this factor is modified by a function which depends on the properties of concrete, namely concrete compressive strength (f_c) and fiber content (C_f). Under this light, fibers are understood to modify the effect of C/D rather than having an effect of their own, assuming that the effect of fibers is not independent from the degree of confinement in geometrical terms or from concrete compressive strength.
- The effect of fibers is assumed to be mainly dependent on fiber content (C_f), but the effect of fiber content is modified by means of a function which depends on fibers geometry, $\nabla_{\mathcal{F}}$. This way, it is considered that the effect of fiber geometry will depend on fiber content, which is a very reasonable assumption.

Estimated coefficients, together with the p-values obtained from the significance tests on these estimates, are shown in Table 4. All the variables and interactions considered in equations (1) and (2) have a statistically significant effect on the risk of splitting, as shown by their p-values (not greater than 0.10 in any case).

5.2 Semi-empirical model obtained to predict splitting failures

If coefficients shown in Table 4 are introduced into equations (1) and (2), the final model for splitting probability is obtained: equation (3) relates splitting probability to the factors and interactions considered, and equation (4) presents the fiber geometry function $\nabla_{\mathcal{F}}$ which modifies the effect of fiber content.

$$ln\left(\frac{p}{1-p}\right) = 8.586 + \left(-12.63 + 0.219 f_c + \nabla_{\mathcal{F}} C_f\right)\frac{C}{D} \quad (3)$$

$$\nabla_{\mathcal{F}} = -0.105 + 0.000325\lambda_f + 0.00174\ell_f \quad (4)$$

This model calculates values for the splitting probability p, but there is one last step so that it can be used to predict splitting cases: a cutoff probability value p* has to be established, so that situations where predicted p is p* or higher correspond to splitting cases, while situations where predicted p are below p* correspond to no splitting cases. The criterion to select this cutoff probability is based on classification efficiency: p* value has to be selected so that the maximum percentage of splitting cases are correctly predicted by the model. After trying different possibilities, the best option is p* = 0.5. This means that predicted probabilities of 0.5 or higher correspond to splitting cases. For all the combinations tested, the splitting probability is calculated and all observations are sorted into two groups: splitting and no-splitting according to the predicted p value. The classification obtained is shown in Table 5. It can be seen that the fitted model proves highly accurate in terms of overall classification capacity (95.1% of all cases are correctly predicted) and particularly in terms of correct prediction of splitting failures (96% of all splitting cases are correctly predicted).

5.3 Effect of compressive strength, C/D ratio and fibers content

Figure 5 shows the values of splitting probability as predicted by the model –equations (3) and (4)– versus C/D and C_f values. This will be referred to as the splitting probability surface hereafter.

It can be observed that higher compressive strength values require higher C/D ratios for splitting failure to be prevented. This can be interpreted as follows: when concrete compressive strength increases, concrete tensile strength is increased and therefore radial stresses developing around the rebar reach further away from it. In consequence, it is more likely that tensile stresses reach the surface of the specimen, this meaning a higher risk of splitting failure. As a result, higher concrete cover values are required when concrete compressive strength is increased.

The horizontal plane in Figure 5 represents the cutoff probability set at $p^*=0.5$ for classification purposes, which distinguishes splitting failures from pullout failures. Accordingly, the intersection between this plane and the splitting probability surface leads to the minimum concrete C/D values that are required to prevent splitting failures, as shown in Figure 6. This requirement varies with fiber content.

The favorable effect of fibers when preventing splitting failures has been revealed to be more important for higher compressive strength values. The reduction in the minimum C/D ratio achieved when adding a certain fiber content to concrete is clearly bigger for 50-MPa concrete than for 35-MPa concrete, as seen in Figure 6.

There is another interesting remark to be made in relation to Figure 6. Since C/D of 5.0 is usually accepted as a good confinement situation, it follows that no splitting of concrete cover should be expected. However, the validity of such an assumption is restricted, as seen in Figure 6: according to the model developed, a POT specimen made with 50-MPa concrete without fibers where C/D is 5.0 is likely to experience a splitting failure.

5.4 Effect of fibers geometry

Figures 7 and 8 illustrate the effect of fibers content and geometry (slenderness in Fig. 7 and length in Fig. 8) together with C/D for a constant concrete compressive strength of 45 MPa.

Figure 7-left shows the splitting probability surface calculated for different values of fiber slenderness for a fiber length of 50mm. The three splitting probability surfaces shown in Figure 7-left are very close to each other. This points out that the effect of

fiber slenderness on the mode of failure of an anchorage, though statistically significant, is not very important in magnitud. The intersection of these surfaces with the horizontal plane p*=0.5 leads to Figure 7-right, where minimum C/D values are shown for different fiber contents and different values of fiber slenderness. It can be concluded that low fiber slenderness values are preferred to prevent splitting of concrete cover.

The effect of fiber length on the mode of bond failure is more complex. Splitting probability surfaces for different fiber length values, assuming a fiber slenderness of 65, are shown in Figure 8-left. Contrarily to what has been observed concerning fiber slenderness, splitting probability surfaces for different fiber length values are clearly distinct. This clearly indicates that the effect of fiber length on the mode of failure of anchorages, besides being statistically significant, is highly relevant. Figure 8-right shows minimum C/D values required to prevent splitting failures after intersection of surfaces in Figure 8-left with the horizontal plane p*=0.5. It is observed that the favorable effect of increasing fiber contents is conditioned to fiber length. The use of long fibers can reverse the trends observed in Figures 5 and 6: when long fibers are used, increasing the fiber content would make the anchorage more prone to splitting and therefore higher C/D values would be required to prevent splitting failures. This would be the case of 60-mm length fibers, as observed in Figure 8-right.

5.5 Exploitation of the model: minimum cover/diameter ratios

The model obtained, given by equations (3) and (4), fits very well the experimental data, as explained in previous sections. However, some problems arise if this model is generalized and extended to values of the different factors outside the range within which they have been tested. This is illustrated in Figure 9, where the experimentally fitted equation is plotted for concrete without fibers. The shaded region defines the situations covered by the experimental results this model is based upon. In that case, there is a vertical asymptote for a concrete compressive strength value of 57.7 MPa. Therefore, the experimentally fitted equation is not valid for compressive strength values higher than 50 MPa. This equation, however, can be modified to overcome this difficulty.

One hypothesis that can be assumed is that the definition of good confinement provided by the Model Code (FIB 2010) is a limit for splitting cases: a C/D value of 5.0 is always enough to prevent splitting failures. If this condition is imposed to the experimentally fitted equation, a continuous, smooth function can be proposed so that it best fits the experimental curve and also the hypothesis arising from the Model Code [8]. This is shown in Figure 9 as "new equation", and for concrete without fibers it is as follows:

$$\frac{C}{D} = \frac{5 + exp\left(\frac{f_c - 30}{3.8}\right)}{4.5 + 0.2exp\left(\frac{f_c - 30}{3.8}\right)} \tag{5}$$

The same has been done for concrete with fibers. Figure 10 shows the curves generalized for different fiber contents, for $\nabla_{\mathcal{F}} C_f$ values between –2.0 and 2.0 (tested values are between –2.5 and 2.5) in addition to unfibered concrete ($\nabla_{\mathcal{F}} C_f$ = 0). This generalized "new equation" is:

$$\frac{C}{D} = \frac{5 + exp\left(\frac{f_c + 5\nabla_{\mathcal{F}} C_f - 30}{3.8}\right)}{4.5 + 0.2exp\left(\frac{f_c + 5\nabla_{\mathcal{F}} C_f - 30}{3.8}\right)} \tag{6}$$

However, following Figures 9 and 10 it is clear that the assumption that a C/D value of 5.0 is always enough to prevent splitting failures is not compatible with the experimental observations reported herein. The curves arising from equations (5) and (6), forced by the horizontal asymptote C/D = 5.0, are excessively diverging from the experimentally fitted equation within the region covered by this experimental programme. Taking into account that the predictive capacity of the model is very high (95.1%), these new formulations introduce an excessive reduction of the model's accuracy. Therefore, the hypothesis that a C/D = 5.0 should always suffice must be rejected because it is in contradiction with experimental results.

An alternative hypothesis can be considered: there might be a C/D value to prevent splitting failures in all cases, but this is not necessarily 5.0. Therefore, a continuous, smooth function other than (5) or (6) can be proposed as long as it meets the following two requirements: a) it must be consistent with the model obtained within the ranges covered by the experimental programme, and b) there must be a horizontal asymptote corresponding to a C/D value higher than 5.0.

Accordingly, the following equation is proposed, and it is plotted in Figure 11 for concrete without fibers and two cases of concrete with fibers:

$$\frac{C}{D} = 1.2 + \frac{(5.6 - 0.2\nabla_{\mathcal{F}} C_f) \cdot exp\left(\frac{f_c + 5\nabla_{\mathcal{F}} C_f - 50}{5}\right)}{0.6 + 0.9exp\left(\frac{f_c + 5\nabla_{\mathcal{F}} C_f - 50}{5}\right)} \tag{7}$$

As can be seen in Figure 11, it follows that the general limit that may be assumed for cover/diameter ratio as well confinement would not be 5.0 but approximately 7.5, although this value needs confirmation in the future by performing new tests.

Equation (7), together with equation (4) for the fiber geometry factor, is a generalized form of the model obtained from experimental observations. This means that it is totally valid within the ranges of values for the different factors tested in the experimental programme, and it has the same accuracy than the model given by equations (3) and (4). Furthermore, it presents no unreasonable discontinuities if it is generalized for values of the factors considered that fall outside the experimental region, and therefore it is adequate to be applied to values slightly different than the ones considered in the experimental programme. However, its validity and accuracy outside this region has to be checked by further experimental campaigns, especially regarding the absolute threshold of C/D = 7.5 and the redefinition of the situation of good confinement from C/D = 5.0 to C/D = 7.5.

6. CONCLUSIONS

- An accurate model for predicting the mode of bond failure has been developed. It relates splitting probability to the values of concrete compressive strength, rebar diameter, concrete cover, fiber content, fiber length, and fiber slenderness. It has been verified that the margin of error is less than 5%.
- Higher compressive strength values require higher concrete cover/diameter ratios for splitting failure to be prevented. When compressive strength of concrete increases, concrete tensile strength is increased and therefore radial stresses developing around the rebar reach further away from it.
- It has been proved that increasing fiber content reduces the risk of splitting failure. The favorable effect of fibers when preventing splitting failures has been revealed to be more important for higher concrete compressive strength values.
- Fiber slenderness and fiber length modify the effect of fiber content on splitting probability and therefore on minimum cover/diameter ratios required to prevent splitting failures.
- Higher fiber slenderness and/or fiber length values imply an increase in bond capacity of concrete and therefore require higher concrete cover values to prevent splitting when developing higher bond stresses.

- The favorable effect of increasing fiber contents is conditioned to fiber length. The use of long fibers can even lead to the fact that increasing fiber contents would make the anchorage more prone to splitting.
- It appears that the definition of the good confinement situations corresponding to cover/diameter = 5.0, as established by the Model Code, is possibly insufficient for SFRCs when concrete compressive strength higher than 50 MPa.

ACKNOWLEDGEMENTS

The authors of this work wish to thank both the Research Bureau of the Spanish Ministry of Science and Innovation and the 'Plan E' programme for the funding of the project 'BIA 2009-12722', this research being a part thereof.

REFERENCES

[1] Cairns J, Plizzari GA. Towards a harmonised European bond test. Materials and Structures 2003;36:498–506.

[2] Bamonte PF, Gambarova PG. High-Bond Bars in NSC and HPC: Study on Size Effect and on the Local Bond Stress-Slip Law. Journal of Structural Engineering 2007;133:225.

[3] Gambarova PG. Bond in reinforced concrete: where do we stand today?, Proceedings of BOND2012 - Bond in Concrete 2012, Brescia, Italy: 2012, pp. 1–13.

[4] Gambarova PG, Rosati GP, Zasso B. Steel-to-concrete bond after concrete splitting: test results. Materials and Structures 1989;22:35–47.

[5] Bazant ZP, Li Z, Thoma M. Identification of stress-slip law for bar or fiber pullout by size effect tests. Journal of Engineering Mechanics 1995;121:620–5.

[6] Bazant ZP, Sener S. Size Effect in Pullout Tests. ACI Materials Journal 1988;85:347–51.

[7] FIB–The International Federation for Structural Concrete. FIB Bulletin No. 10: Bond of reinforcement in concrete. Lausanne, Switzerland, 2000, 434 pp.

[8] FIB–The International Federation for Structural Concrete. Model Code 2010. Published by Ernst & Sohn, 2013, 434 pp.

[9] Cairns J, Jones K. The splitting forces generated by bond. Magazine of Concrete Research 1995;47:153–65.

[10] ACI Committee 318, 2011. ACI 318-11: Building Code Requirements for Structural Concrete and Commentary. Ed. by American Concrete Institute (ACI), Farmington Hills, Michigan, United States, 503 pp.

[11] Yalciner H, Eren O, Sensoy S. An experimental study on the bond strength between reinforcement bars and concrete as a function of concrete cover, strength and corrosion level. Cement and Concrete Research 2012;42:643–55.

[12] Arel HS, Yazici S. Concrete-reinforcement bond in different concrete classes. Construction and Building Materials 2012;36:78–83.

[13] García-Taengua E, Martí-Vargas JR, Serna-Ros P. Statistical Approach to Effect of Factors Involved in Bond Performance of Steel Fiber-Reinforced Concrete. ACI Structural Journal 2011;108:461–8.

[14] Cairns J, Plizzari GA. Bond behaviour of conventional reinforcement in fibre reinforced concrete, Varenna, Italy: 2004.

[15] Holschemacher K, Weisse D. Bond of reinforcement in fibre reinforced concrete, Varenna, Italy: 2004.

[16] García-Taengua E, Arango S, Martí-Vargas JR, Serna P. Flexural Creep of Steel Fiber Reinforced Concrete in the Cracked State. Construction and Building Materials 2014, DOI 10.1016/j.conbuildmat.2014.04.139

[17] Dancygier AN, Katz A, Wexler U. Bond between deformed reinforcement and normal and high-strength concrete with and without fibers. Materials and Structures 2010;43:839–56.

[18] Ministerio de Fomento, 2008. Instrucción Española de Hormigón Estructural EHE-08, Madrid, Spain, 304 pp.

[19] ACI Committee 408, 2003. Report ACI 408R-03: Bond and Development of Straight Reinforcing Bars in Tension. Ed. by American Concrete Institute (ACI), Farmington Hills, Michigan, United States, 49 pp.

[20] Serna P, Arango S, Ribeiro T, Núñez A, García-Taengua E. Structural cast-in-place SFRC: technology, control criteria and recent applications in spain. Materials and Structures 2009;42:1233–46.

[21] Shah AA, Ribakov Y. Recent trends in steel fibered high-strength concrete. Materials & Design 2011;32:4122–51.

[22] Arango SE, Serna P, Martí-Vargas J, García-Taengua E. A Test Method to Characterize Flexural Creep Behaviour of Pre-cracked FRC Specimens. Experimental Mechanics 2012;52:1067–78.

[23] Darwin D, Zuo J. Development Length Criteria for Conventional and High Relative Rib Area Reinforcing Bars. ACI Structural Journal 1996;93:347–59.
[24] Lundgren K, Gylltoft K. A Model for the Bond between Concrete and Reinforcement. Magazine of Concrete Research 2000;52:53–63.
[25] Harajli MH, Mabsout ME. Evaluation of Bond Strength of Steel Reinforcing Bars in Plain and Fiber-Reinforced Concrete. ACI Structural Journal 2002;99:509–17.
[26] Russo G, Pauletta M. A simple method for evaluating the maximum slip of anchorages. Materials and Structures 2006;39:533–46.
[27] Russo G, Pauletta M, Mitri D. Solution for bond distribution in asymmetric R.C. structural members. Engineering Structures 2009;31:633–41.
[28] Tastani SP, Pantazopoulou SJ. Direct Tension Pullout Bond Test: Experimental Results. Journal of Structural Engineering 2010;136:731–43.
[29] Harajli MH. Bond Stress–Slip Model for Steel Bars in Unconfined or Steel, FRC, or FRP Confined Concrete under Cyclic Loading. Journal of Structural Engineering 2009;135:509–18.
[30] Cattaneo S, Rosati G. Bond between Steel and Self-Consolidating Concrete: Experiments and Modeling. ACI Structural Journal 2009;106:540–50.
[31] Harajli MH, Hout M, Jalkh W. Local Bond Stress-Slip Behavior of Reinforcing Bars Embedded in Plain and Fiber Concrete. ACI Materials Journal 1995;92:343–54.
[32] RILEM-CEB-FIP, 1970. Bond test for reinforcing steel: 2. Pull-Out Test. Materials and Structures, 3(3), pp.175–178.
[33] RILEM, 1983 (1994), RC6–Bond test for reinforcement steel. 2. Pull-out test. RILEM Recommendations for the Testing and Use of Constructions Materials, pp. 218-220, ed. by E & FN SPON.
[34] Gambarova PG, Rosati G. Bond and splitting in reinforced concrete: test results on bar pull-out. Materials and Structures 1996;29:267–76.
[35] EN 1992-1-1, 2004. Eurocode 2: Design of Concrete Structures – Part 1- 1: General Rules and Rules for Buildings. Ed. by European Committee for Standardization, Brussels, Belgium, 225 pp.
[36] Montgomery, D., Design & Analysis of Experiments, sixth edition, John Wiley & Sons, Inc., New York, 2005, 643 pp.
[37] Kleinbaum, D.G., & Klein, M., 2010. Logistic Regression: A Self-Learning Text (3rd ed.). Ed. by Springer, New Jersey, United States, 701 pp.

FIGURES

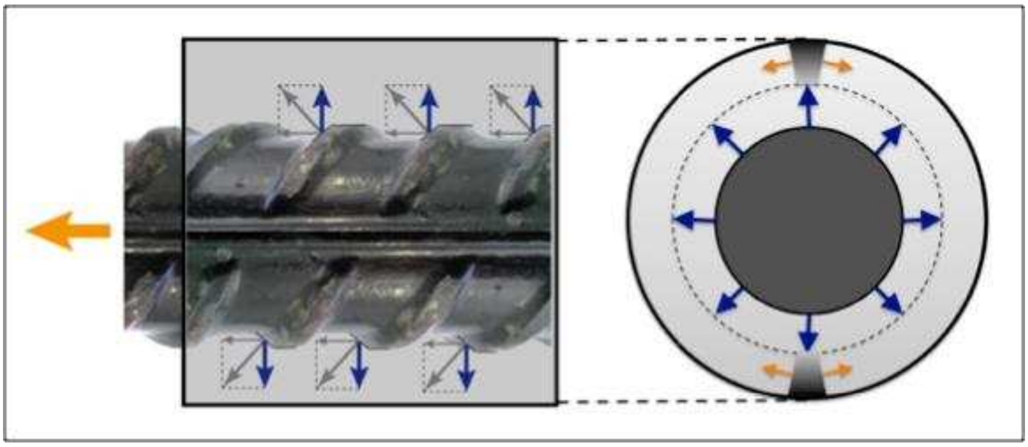

Figure 1. Bond stresses and radial stresses generated at the rebar-concrete interface.

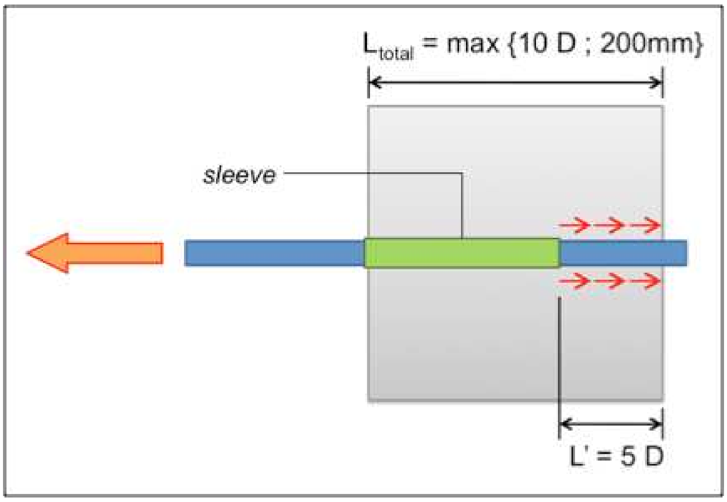

Figure 2. Longitudinal view of POT specimen according to RILEM recommendations.

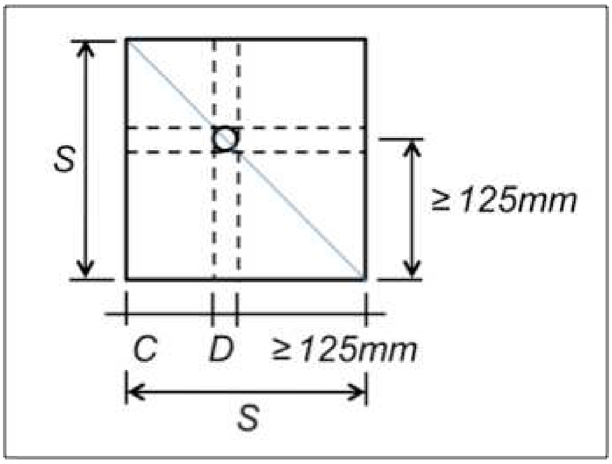

Figure 3. Cross-section of POT specimens.

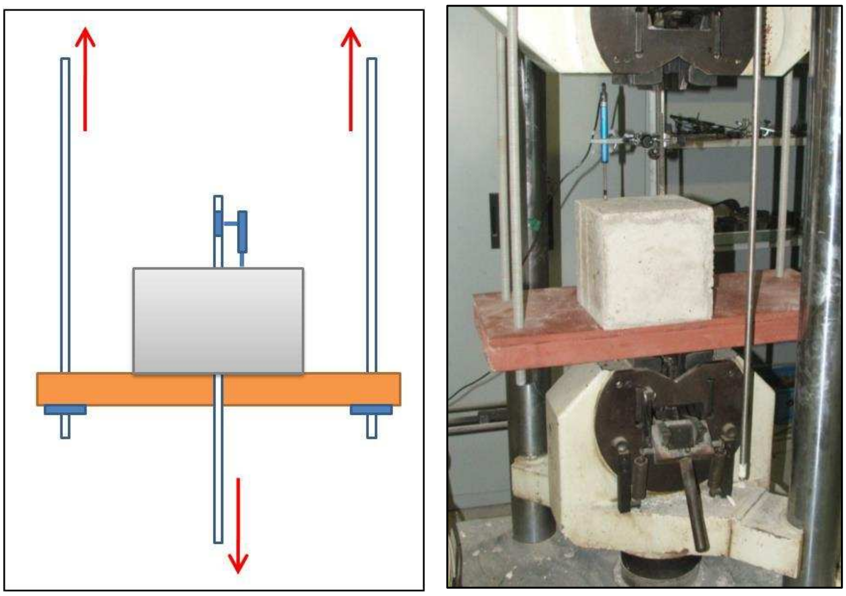

Figure 4. Force diagram (left) and a view of the pull out test as performed in this research (right).

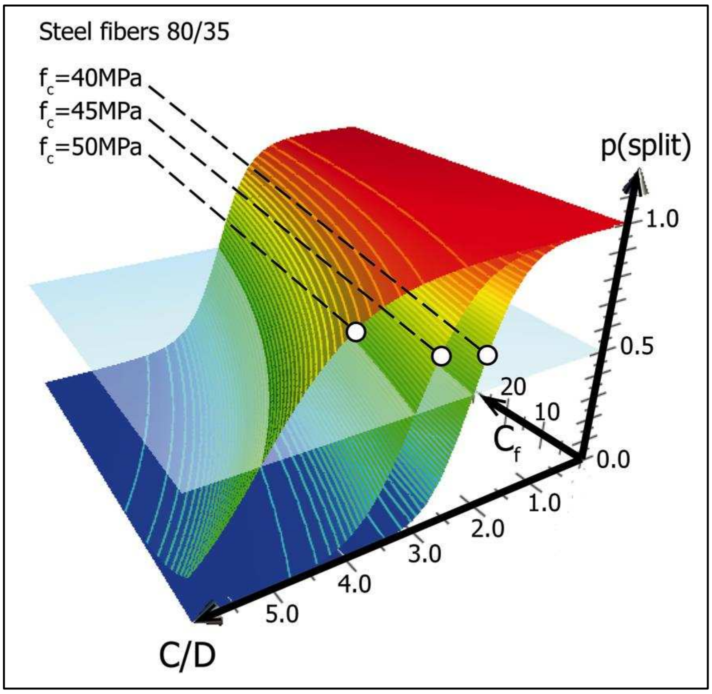

Figure 5. Splitting probability surfaces for concrete between 40MPa and 50MPa reinforced with 80/35 steel fibers.

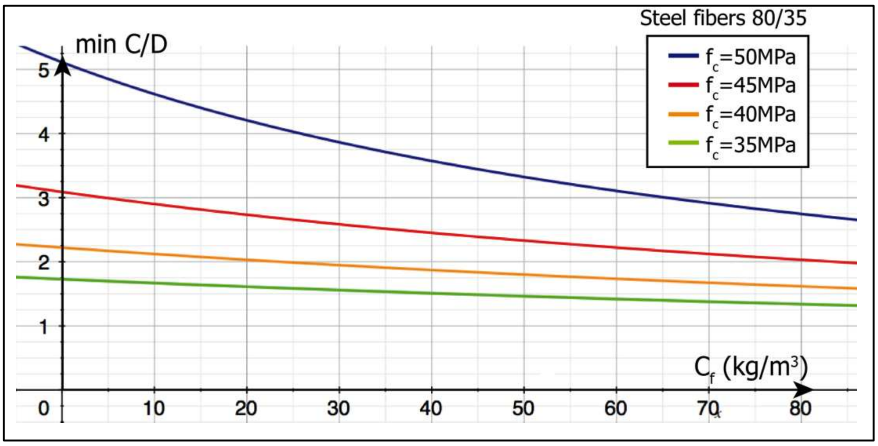

Figure 6. Minimum C/D values to avoid splitting failure of concrete reinforced with 80/35 steel fibers.

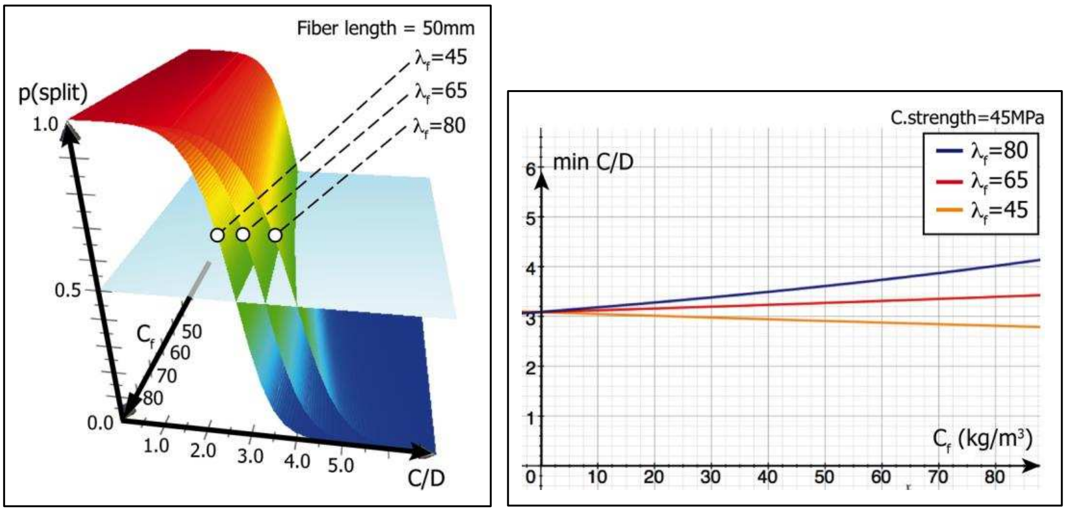

Figure 7. Splitting probability surfaces (left), and minimum C/D values to avoid splitting failure for 45-MPa concrete reinforced with 50-mm fibers (right).

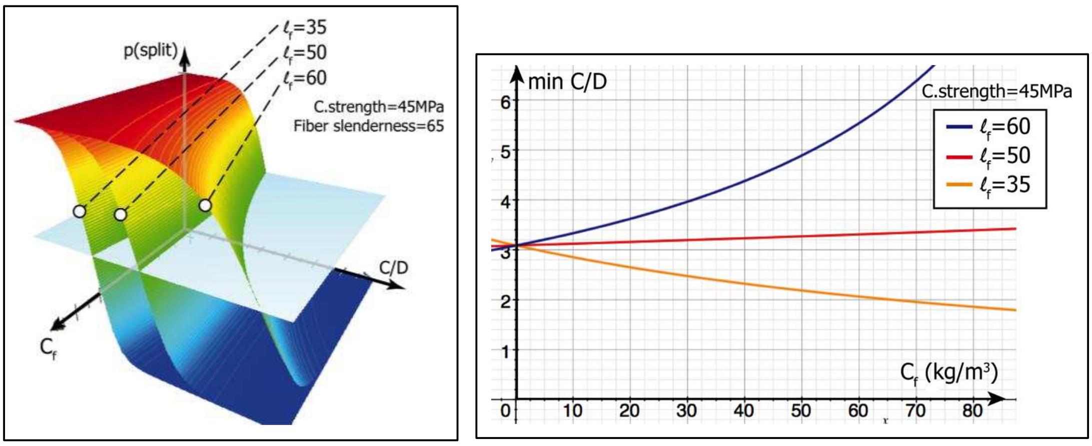

Figure 8. Splitting probability surfaces (left) and minimum C/D values to avoid splitting failure, for 45-MPa concrete reinforced with fibers of slenderness 65.

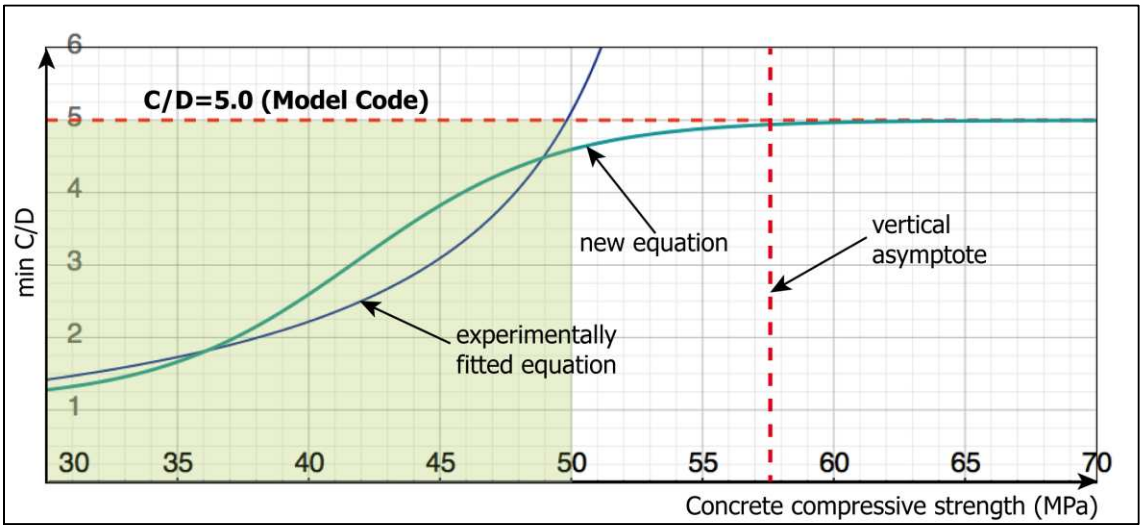

Figure 9. Function to relate min C/D to compressive strength (optimum C/D=5.0 according to Model Code)

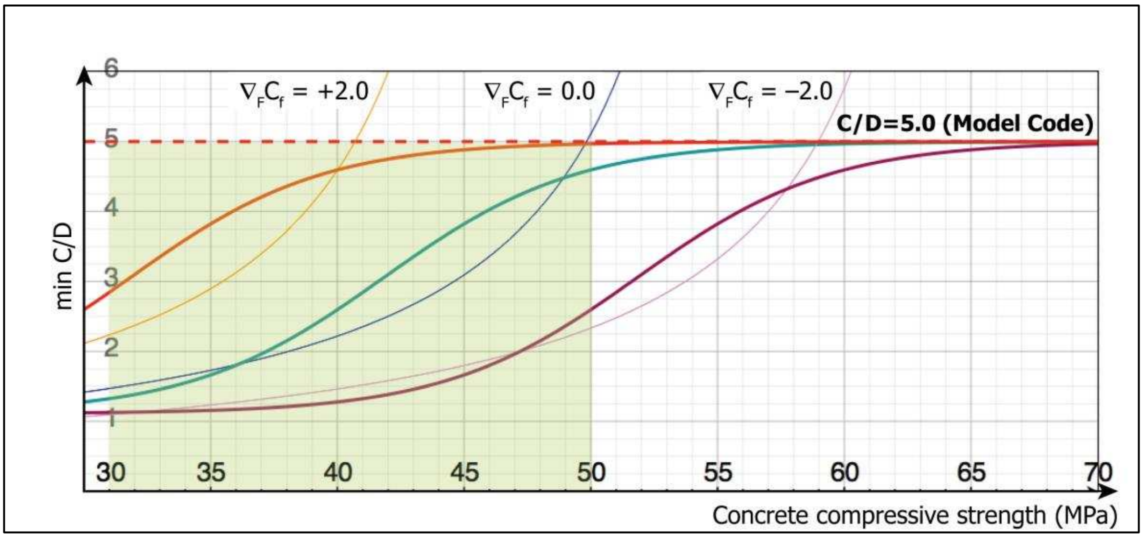

Figure 10. Generalized function to relate min C/D to compressive strength (optimum C/D=5.0 according to Model Code).

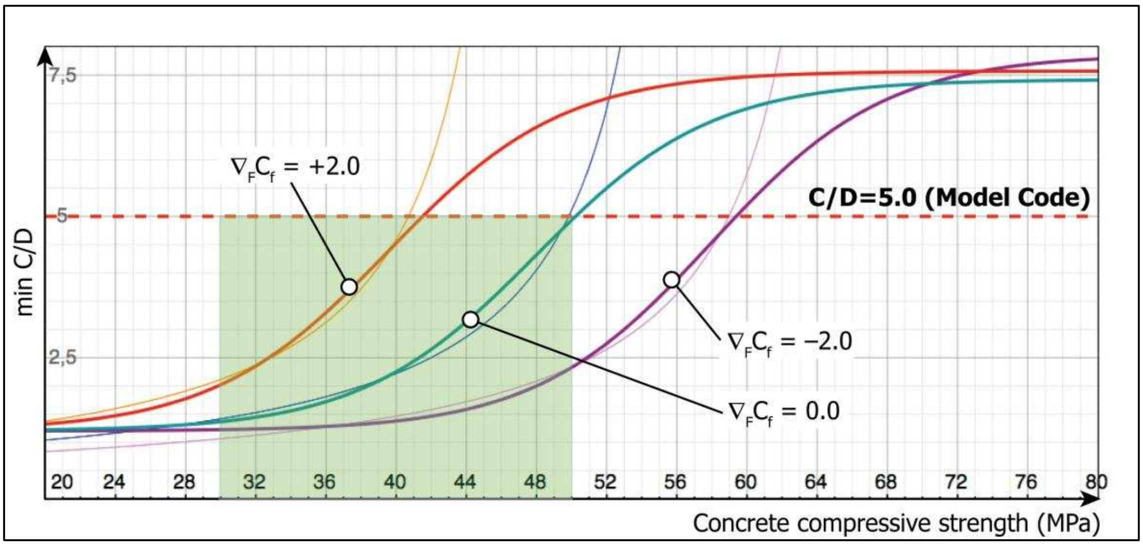

Figure 11. Generalized function to relate min C/D to compressive strength (Model Code optimum C/D=5.0 not assumed).

TABLES

Table 1. Factors and levels considered.

	Type I mixes	Type II mixes	Type III mixes
Rebar diameter, mm	8 16 20	8 12 16	8 12 16
Concrete cover	C1=30mm C2= (C1+C3)/2 C3=5 D	C1=2.5 D C2=3.5 D C3=5.0 D	C1=2.5 D C2=3.5 D C3=5.0 D
Fiber geometry (slenderness / length)	65/60 80/50	45/50 80/50 80/35	45/50 80/50 80/35
Fiber content, kg/m^3	0 40 70	0 40 60	0 40 60

Table 2. Reference mix designs (kg/m^3).

	Type I	Type II	Type III
Water/Cement	0.60	0.45	0.55
Cement	325	440	325
Sand 0/4	1006	957	1050
Coarse aggr. 7/12	544	723	835
Coarse aggr. 12/20	362	-	-
Filler	-	72	37
Superplasticizer	1.40	10	1.40

Table 3. Combinations tested and number of splitting cases observed.

Combination	Fibers geometry (λ_f / l_f)	Fiber content (kg/m^3)	Rebar diameter (mm)	Concrete Cover	Bond strength (MPa)	Splitted specimens
I-1	65/60	40	16	C1	6.24	0
I-2	-	0	8	C2	8.36	0
I-3	65/60	70	20	C3	18.44	0
I-4	65/60	40	8	C3	7.78	0
I-5	-	0	20	C1	--	3/3
I-6	65/60	70	16	C2	6.83	0
I-7	80/50	40	20	C2	11.79	0
I-8	-	0	16	C3	5.76	0
I-9	80/50	70	8	C1	5.62	0
II-1	-	0	8	C1	15.52	1/3
II-2	80/35	60	8	C2	31.12	0
II-3	45/50	40	8	C3	21.35	0

II-4	45/50	60	12	C1	--	3/3
II-5	80/50	40	12	C2	23.90	2/3
II-6	-	0	12	C3	25.29	0
II-7	80/35	40	16	C1	--	3/3
II-8	-	0	16	C2	--	3/3
II-9	80/50	60	16	C3	--	3/3
III-1	-	0	8	C1	--	3/3
III-2	80/50	40	12	C2	14.37	0
III-3	80/50	60	16	C3	21.95	0
III-4	-	0	12	C3	13.83	0
III-5	45/50	40	16	C1	--	3/3
III-6	45/50	60	8	C2	22.00	0
III-7	-	0	16	C2	21.15	1/3
III-8	80/35	40	8	C3	14.03	0
III-9	80/35	60	12	C1	20.98	0

Table 4. Estimated coefficients and significance tests for the semi-empirical model obtained for splitting probability.

		Coefficient	p-value
(constant)	∇_0	8.58577	--
Cover/Diameter, C/D	∇_{cd}	-12.629	0.0000
Compr. Strength, $\boldsymbol{f_c}$ C/D	∇_c	0.219206	0.0000
Fiber Content, $\boldsymbol{C_f}$ C/D	∇_f	-0.105321	0.0004
Fiber Slenderness, $\boldsymbol{\lambda_f C_f}$ C/D	$\nabla_{\lambda f}$	0.00032465	0.0799
Fiber Length, $\boldsymbol{\ell_f C_f}$ C/D	$\nabla_{\ell f}$	0.0017429	0.0003

Table 5. Classification table, threshold probability of 0.5 (semi-empirical model).

Observed		Predicted		Percentage correct
		pullout	splitting	
pullout	56	53	3	53/56= 94.6%
splitting	25	1	24	24/25= 96.0%
Total: 56 + 25 = 81 specimens				overall (53 + 24)/81= 95.1%